C. H. M. Broeders and A. Yu. Konobeyev

Phenomenological model for non-equilibrium deuteron emission in nucleon induced reactions

A new approach is proposed for the calculation of non-equilibrium deuteron energy distributions in nuclear reactions induced by nucleons of intermediate energies. It combines the model of the nucleon pick-up, the coalescence and the deuteron knock-out. Emission and absorption rates for excited particles are described by the preequilibrium hybrid model. The model of Sato, Iwamoto, Harada is used to describe the nucleon pick-up and the coalescence of nucleons from the exciton configurations starting from (2p, 1h). The model of deuteron knock-out is formulated taking into account the Pauli principle for the nucleon-deuteron interaction inside a nucleus. The contribution of the direct nucleon pick-up is described phenomenologically. The multiple pre-equilibrium emission of particles is taken into account. The calculated deuteron energy distributions are compared with experimental data from ^{12}C to ^{209}Bi.

Phänomenologisches Modell für die Nicht-Gleichgewichts-Energieverteilungen für Deuteronen aus Kern-Reaktionen. *Es wird ein neuer Ansatz vorgeschlagen für die Berechnung der Nicht-Gleichgewichts-Energie-Verteilungen für Deuteronen aus Kern-Reaktionen verursacht durch Nukleonen mit mittleren Energien. Dieser Ansatz kombiniert das Nukleon Pick-up Modell, Koaleszenz und Deuteron Knock-out. Die Emissions- und Absorptionsraten für angeregte Teilchen werden mit dem Preequilibrium Hybrid Modell beschrieben. Für die Beschreibung des Nukleon Pick-ups und der Koaleszenz von Nukleonen aus den Exciton Konfigurationen ab (2p, 1h) wird das Modell von Sato, Iwamoto, Harada benutzt. Bei der Formulierung des Modells für Deuteron Knock-out wird für die Nukleon-Deuteron Wechselwirkung im Nukleus das Pauli-Prinzip berücksichtigt. Der Beitrag des direkten Nukleonen Pick-ups wird Phänomenologisch beschrieben. Die mehrfache Preequilibrium Emission von Teilchen wird berücksichtigt. Die berechneten Energie-Verteilungen für Deuteronen werden verglichen mit experimentellen Daten von ^{12}C bis ^{209}Bi.*

1 Introduction

Ten years ago a paper [1] was published concerning the precompound deuteron emission in nuclear reactions induced by nucleons of intermediate energies. The model proposed has been one of the first applications of the coalescence pick-up model [2, 3] and the first application of the hybrid model [4] to the description of the non-equilibrium deuteron emission in nuclear reactions.

The model [1] was in a peculiar competition with the model of the complex particle emission [5] formulated basing on the theory of the pre-equilibrium particle emission. During long time both models [1, 5] were used for the qualitative description of deuteron spectra in nucleon induced reactions. The need in reliable nuclear data at primary nucleon energies up to 150 MeV [6, 7] in a new way raised a question about the accuracy of model calculations. The requirement of quantitative description of nuclear reaction characteristics has acquired a special importance. The pre-equilibrium exciton model [5] has been renewed in Ref. [8] and the success of the improved model in the calculation of complex particle emission spectra has been demonstrated in Refs. [9–11].

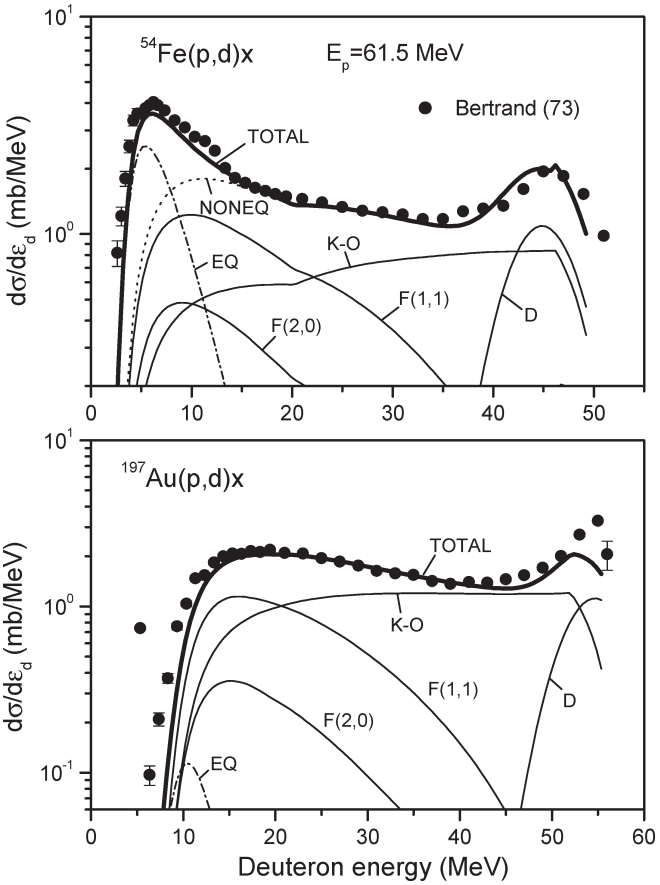

Fig 1. The contribution of different nuclear processes in the deuteron emission in reactions $p + ^{54}Fe$ and $p + ^{197}Au$ induced by 61.5 MeV protons: the equilibrium emission (EQ), the pick-up of nucleon from the exciton states starting from (2p, 1h) (F(1,1)), the coalescence of two excited nucleons (F(2,0)), the direct pick-up (D). Also the sum of all non-equilibrium components (NONEQ) and the total spectrum (TOTAL) are shown. The nonequilibrium deuteron spectrum for $p + ^{197}Au$ reaction almost coincides with the total spectrum (see Fig. 6). Experimental data (black circles) are taken from Ref. [12]. The deuteron energy is shown in laboratory coordinate system as in other Figures of the paper

The present work concerns the further development of the approach [1] formulated basing on the exciton coalescence pick-up model [3] and the hybrid model [4].

2 Model description

Both approaches [1, 5] describing the non-equilibrium deuteron emission neglect of the final size of the nuclear potential well. Taking it into account, one obtains that the level density of the final state corresponding to the direct nucleon pick-up, ω(0p, 1h, U) [1, 5] is different from zero only at the energy of the residual excitation below the Fermi energy. It immediately results to a noticeable discrepancy of measured data and deuteron emission spectra calculated by both approaches [1, 5]. Formally, the pick-up component with the (0p, 1h) final state can be referred to the high energy tail of the deuteron emission spectrum, which usually has a peak in the measured energy distribution [12, 13]. The DWBA calculation [14] confirms this qualitative consideration.

This fact makes it necessary to search for other principles for the formulation of the pre-equilibrium model of the deuteron emission. Return to the coalescence model of Ribanský, Obložinský [15], which is used up to now for the analysis of complex particle emission [16], cannot be fully justified for reasons discussed and investigated in details in Refs. [2, 3]. Most likely, it is necessary to search for the solution in a combination of the models describing different nuclear processes resulting to the deuteron emission, which physical validity meets no serious objections.

In the present work, it is supposed that the non-equilibrium deuteron emission in nucleon induced reactions results from: i) the pick-up of nucleon with the energy below the Fermi energy (E_F) after the formation of the (2p, 1h) initial exciton state, ii) the coalescence of two excited nucleons with energies above E_F, iii) the knock-out of the "preformed" deuteron, iv) the direct process resulting in the deuteron formation and escape. The non-equilibrium deuteron spectrum is calculated as a sum of different components

$$\frac{d\sigma}{d\varepsilon_d} = \frac{d\sigma^{P-U,C}}{d\varepsilon_d} + \frac{d\sigma^{K-O}}{d\varepsilon_d} + \frac{d\sigma^{D}}{d\varepsilon_d}, \quad (1)$$

where the first term relates to the pick-up and the coalescence after the formation of the (2p, 1h) exciton state, the second component describes the contribution of the deuteron knock-out and the last term relates to the direct process.

The analytical expressions for each component of the deuteron emission spectrum were obtained using basic statements of the hybrid model [4] (Sect. 2.1–2.4).

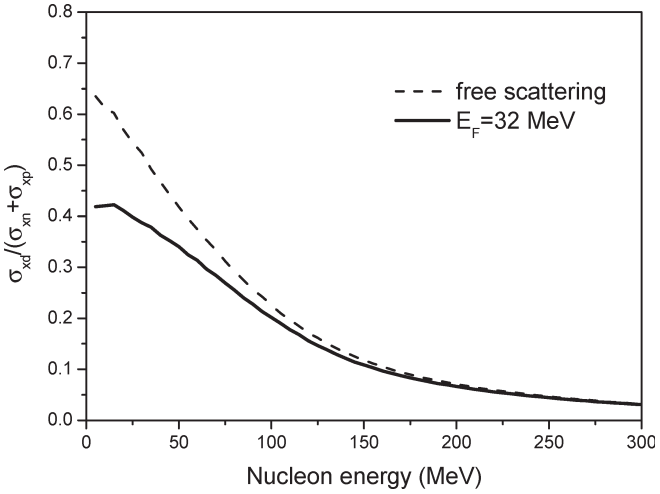

Fig. 2. The ratio of the elastic nucleon-deuteron scattering cross-section to the sum of the elastic nucleon-nucleon cross-sections $\sigma_{xd}/(\sigma_{xp}+\sigma_{xn})$ calculated for the nuclear potential well with the Fermi energy equal to 32 MeV (solid line) and for the free scattering (dashed line). Incident nucleon kinetic energy is outside the nucleus (x-axis)

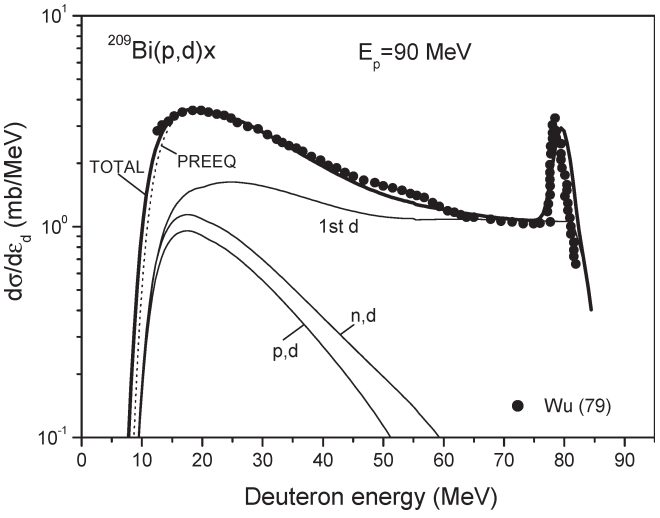

Fig. 3. The contribution of deuterons formed on different pre-equilibrium stages of the nuclear reaction p + ^{209}Bi induced by 90 MeV protons in the total deuteron emission spectrum: the emission of the first pre-compound deuteron ("1st d"), the pre-compound deuteron emission after the pre-equilibrium proton escape ("p,d"), the pre-compound deuteron emission following the pre-equilibrium neutron emission ("n,d"). The sum of all pre-equilibrium components ("1st d" + "p,d" + "n,d") (PREEQ) and the total spectrum (TOTAL) are shown. Experimental data (black circles) are taken from Ref. [13]

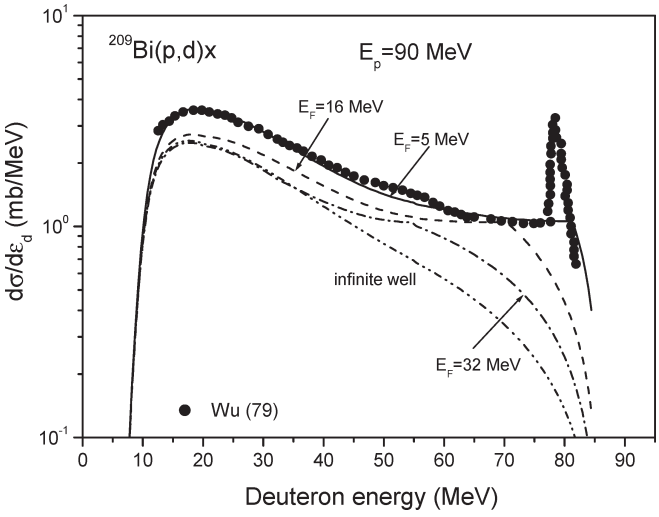

Fig. 4. The deuteron emission spectrum for ^{209}Bi(p,d)x reaction induced by 90 MeV protons calculated using different value of the effective Fermi energy E_F. Experimental data (black circles) are taken from Ref. [13]

The exciton level density is calculated following Běták and Dobeš [17] taking into account the finite depth of the nuclear potential well

$$\omega(p,h,E) = g^p \tilde{g}^h \sum_{k=0}^{h} {}_hC_k (-1)^k \Theta(E - kE_F) \frac{(E - kE_F)^{n-1}}{p!h!(n-1)!} \quad (2)$$

where *"p"* is the number of particles; *"h"* is the number of holes; *"n"* is equal to the sum of *"p"* and *"h"*; E is the energy of the excitation; E_F is the Fermi energy; g and $\tilde{g}$ are the single level density for particles and holes, respectively; $\Theta(x)$ is the Heaviside function, $\Theta = 0$ for $x < 0$ and $\Theta = 1$ for $x > 0$.

The single level density for particles and holes are calculated according to Ref. [17]

$$g = A/14, \quad (3)$$

$$\tilde{g} = A/E_F \quad (4)$$

The surface nucleus effects [18, 19] make an influence on the effective value of the Fermi energy E_F used for the calculation of precompound particle spectra. It is discussed in Sect. 2.5.

2.1 Pick-up and coalescence

The exciton coalescence pick-up model proposed in Refs.[2,3] is used for the calculation of the $d\sigma^{P-U,C}/d\varepsilon_d$ spectrum component [1]

$$\frac{d\sigma^{P-U,C}}{d\varepsilon_d} = \sigma_{non}(E_0) \sum_{n=n_0} \sum_{k+m=2} F_{k,m}(\varepsilon_d + Q_d) \times \frac{\omega(p-k,h,U)}{\omega(p,h,E)} \frac{\lambda_d^e(\varepsilon_d)}{\lambda_d^e(\varepsilon_d) + \lambda_d^+(\varepsilon_d)} g_d D(n), \quad (5)$$

where σ_{non} is the cross-section of nonelastic interaction of the nucleus and the primary particle with the kinetic energy E_0; $F_{k,m}$ is the deuteron formation factor equal to the probability that the deuteron is composed of *"k"* particles above the Fermi level and *"m"* particles below; the residual excitation energy U is equal to $E - Q_d - \varepsilon_d$, *and* E is the excitation energy of the composite nucleus, Q_d is the separation energy for the deuteron; ε_d is the channel emission energy corresponding to the deuteron emission; λ_d^e is

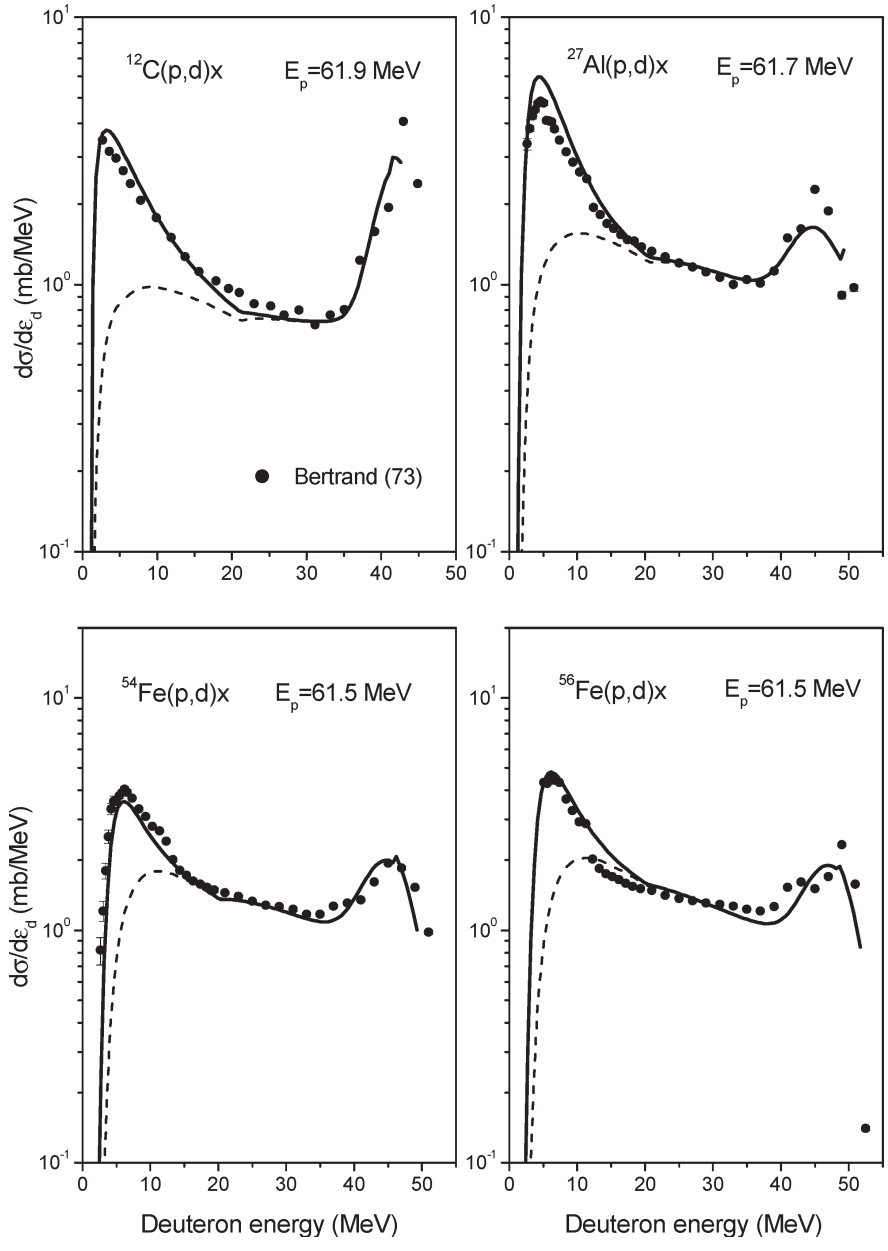

Fig. 5. Calculated total deuteron emission spectrum (solid line) and nonequilibrium deuteron emission spectrum (dashed line) for ^{12}C, ^{27}Al, ^{54}Fe and ^{56}Fe irradiated with 61.5–61.9 MeV protons. Experimental data are from Ref. [12]

the deuteron emission rate; λ_d^+ is the intranuclear transition rate for the absorption of the formed deuteron in the nucleus; g_d is the density of single states for the deuteron; $D(n)$ is the factor describing the "depletion" of the n-exciton state due to the particle emission; n_0 is the initial exciton number, $(n_0 = 3)$.

The deuteron emission rate is calculated with the following formula

$$\lambda_d^e = \frac{(2S_d + 1)\mu_d \varepsilon_d \sigma_d^{inv}(\varepsilon_d)}{\pi^2 \hbar^3 g_d}, \tag{6}$$

where S_d and μ_d are spin and reduced mass of the outgoing deuteron; σ_d^{inv} is the inverse reaction cross-section for deuteron. The deuteron absorption rate is equal to

$$\lambda_d^+ = 2W_d^{opt}/\hbar, \tag{7}$$

where W_d^{opt} is the imaginary part of the optical potential for deuteron.

The form factors of the deuteron formation $F_{k,m}$ were calculated in Ref. [3] for the effective nuclear radius with the dR parameter value equal to 1 fm. The original values [3] are approximated and presented as follows

$$F_1, 1(e) = \begin{cases} -1.409 \cdot 10^{-2}\varepsilon + 0.6 & for\, \varepsilon \le 30\, MeV \\ 1.377 \cdot 10^{-4}\,\varepsilon^2 - 1.807 \cdot 10^{-2}\,\varepsilon + 0.5946 & for\, 30 < \varepsilon \le 65\, MeV, \\ 0 & for\, \varepsilon > 65\, MeV \end{cases} \tag{8}$$

$$F_{2,0}(\varepsilon) = 0.6 - Z_{1,1}(\varepsilon) \tag{9}$$

As an illustration, Fig. 1 shows the pick-up and coalescence contribution in the deuteron emission spectrum for ^{54}Fe and ^{197}Au irradiated with 61.5 MeV protons.

2.2 Knock-out

The deuteron knock-out process has been studied in Ref. [20] relating to (n, d) reaction cross-section. The present work concerns the possible contribution of the knock-out in deuteron emission spectra. By the analogy with the α-particle emis-

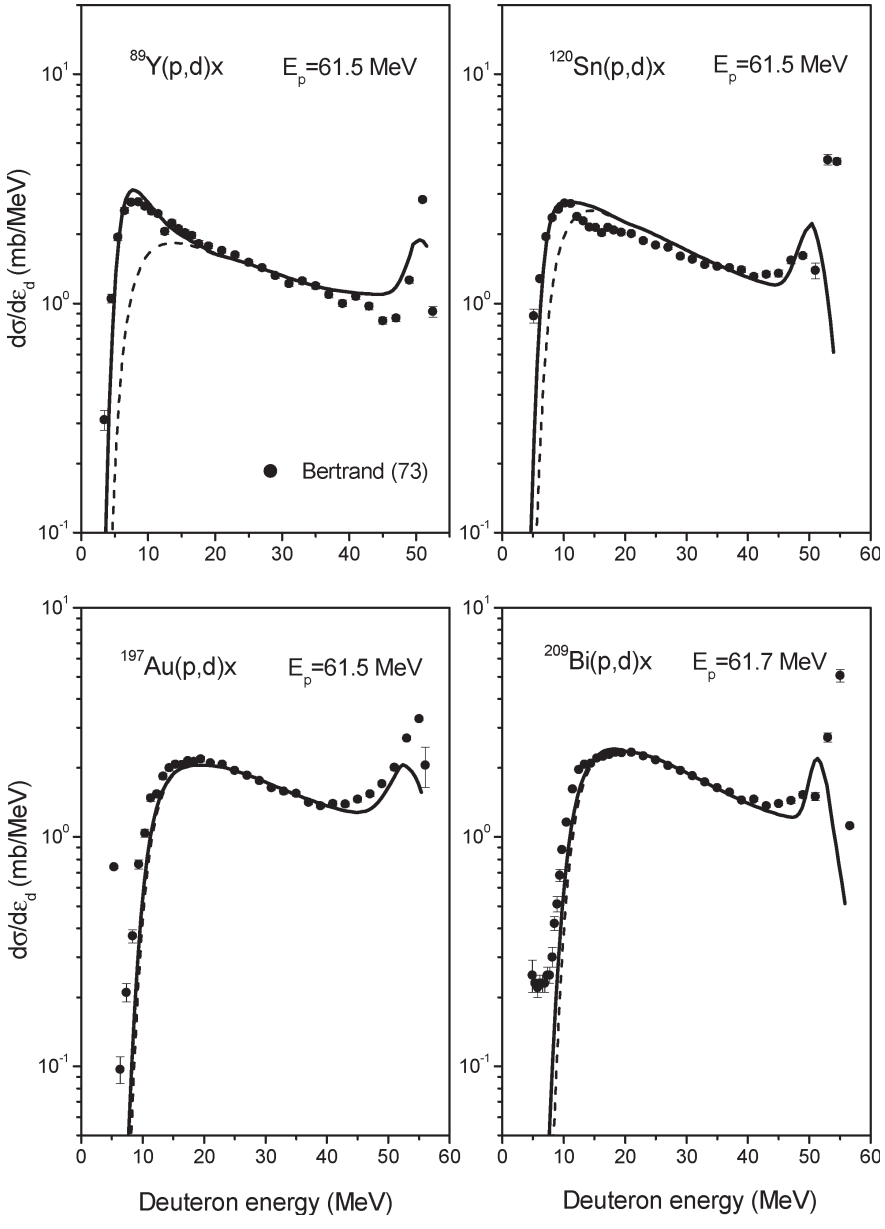

Fig. 6. Calculated total deuteron emission spectrum (solid line) and nonequilibrium deuteron emission spectrum (dashed line) for ^{89}Y, ^{120}Sn, ^{197}Au and ^{209}Bi reactions induced by 61.5 MeV protons. Experimental data are from Ref. [12]

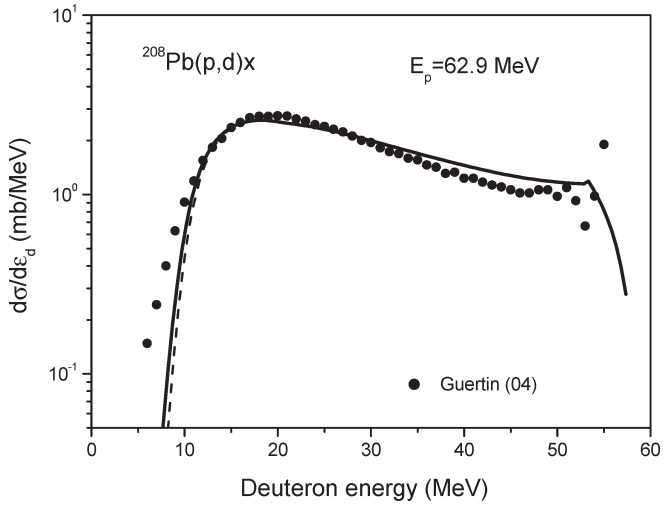

Fig. 7. Calculated total deuteron emission spectrum (solid line) and nonequilibrium deuteron emission spectrum (dashed line) for the ^{208}Pb(p,d)x reaction induced by 62.9 MeV protons. Experimental data are taken from Ref. [27]

sion [21, 22] the knock-out component of the precompound deuteron emission spectrum is written as follows

$$\frac{d\sigma^{K-O}}{d\varepsilon_d} = \sigma_{non}(E_0) \sum_{n=n_0} \Phi_d(E_0) \frac{g}{g_d p}$$

$$\times \frac{\omega(p-1,h,U)}{\omega(p,h,E)} \frac{\lambda_d^e(\varepsilon_d)}{\lambda_d^e(\varepsilon_d) + \lambda_d^+(\varepsilon_d)} g_d D(n), \quad (10)$$

where the factor $g/(g_d p)$ justifies the substitution of the level density $\omega(\pi, \tilde{\pi}, \nu, \tilde{\nu}, d, \tilde{d}, E)$ for the three-component system (neutron, proton, deuteron) [23, 21] by the one-component state density $\omega(p, h, E)$ in Eq. (10). The factor Φ_d describes the initial number of excited deuteron clusters in the nucleus

$$\Phi_d = 2F_d(E_0), \quad (11)$$

where F_d is the probability of interaction of the incident particle with the "preformed" deuteron resulting in its excitation in the nucleus; factor of two reflects the normalization on the number of particles in the initial exciton state n_0.

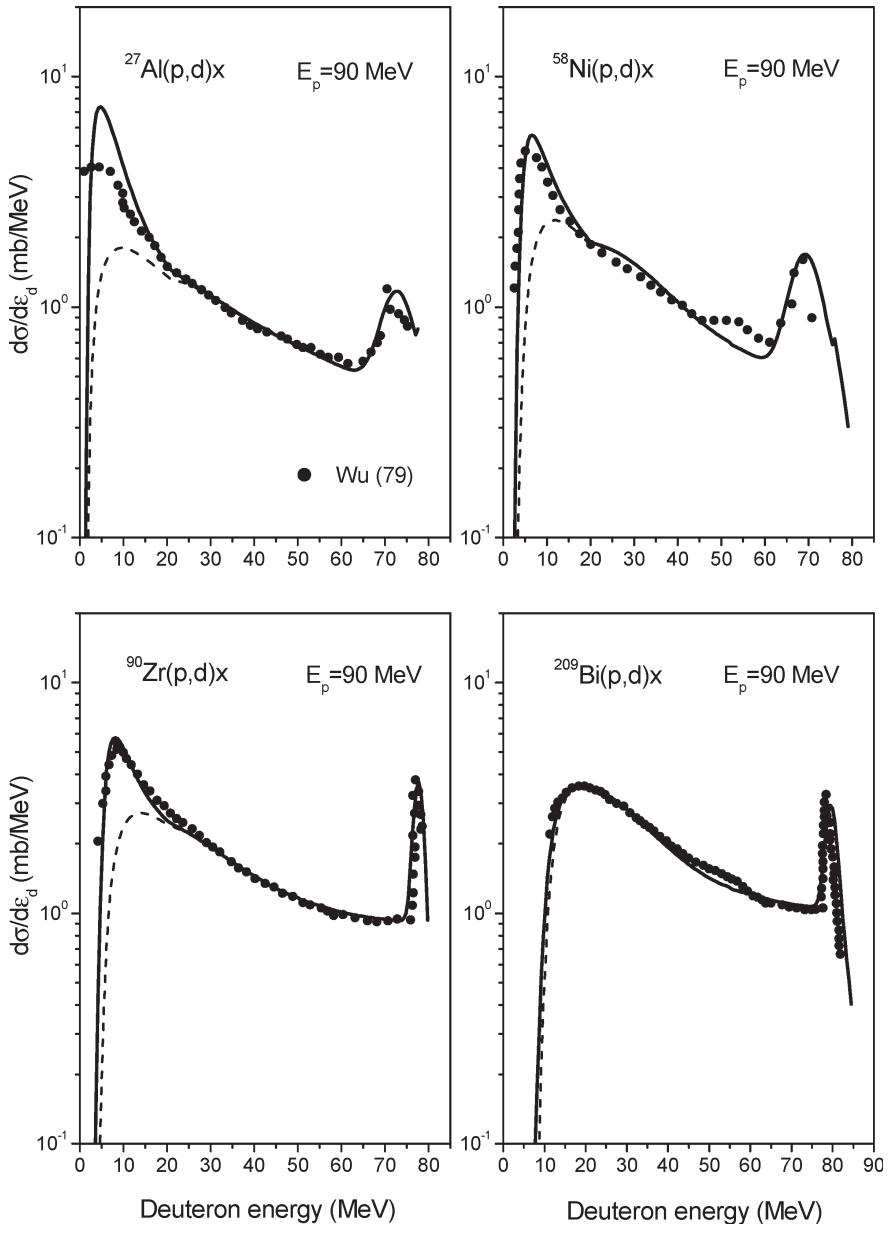

Fig. 8. Calculated total deuteron emission spectrum (solid line) and nonequilibrium deuteron emission spectrum (dashed line) for ^{27}Al, ^{58}Ni, ^{90}Zr and ^{209}Bi irradiated with 90 MeV protons. Experimental data are taken from Ref. [13]

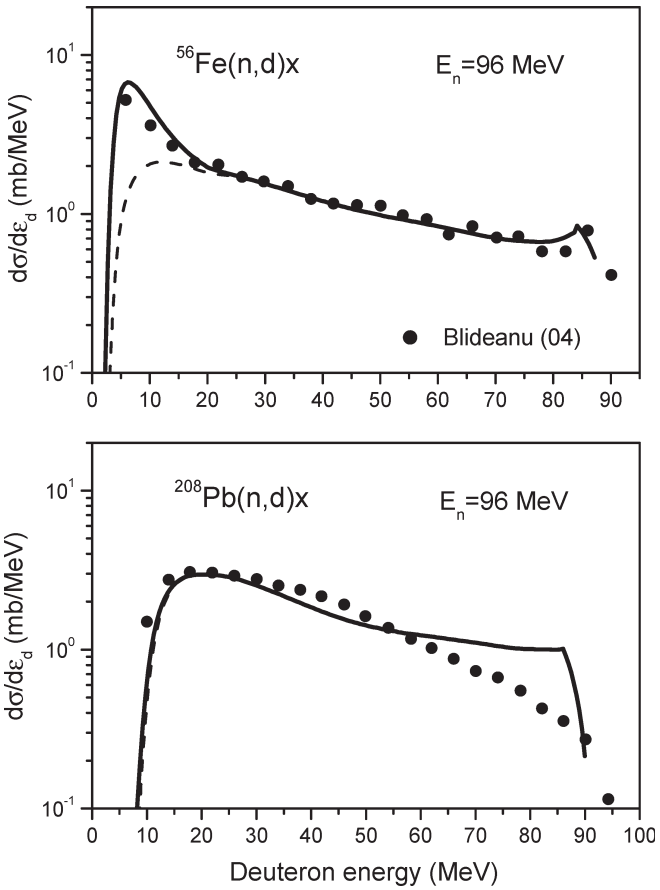

Fig. 9. Calculated total deuteron emission spectrum (solid line) and nonequilibrium deuteron emission spectrum (dashed line) for ^{56}Fe and ^{208}Pb irradiated with 96 MeV neutrons. Experimental data are taken from Ref. [16]

The general expression for F_d is

$$F_d = \frac{\varphi\sigma_{xd}(E_0)}{\frac{Z'}{A'}\sigma_{xp}(E_0) + \frac{(A-Z)}{A}\sigma_{xn}(E_0) + \varphi\sigma_{xd}(E_0)}, \tag{12}$$

where *"x"* refers to the initial proton or neutron; σ_{xd}, σ_{xp} and σ_{xn} are the cross-sections of the elastic interaction of projectile with deuteron, proton and neutron, respectively corrected for a Pauli principle; φ is the number of "preformed" deuterons in the nucleus; Z' and A' are number of protons and nucleons in the nucleus corrected for a number of deuterons clustered.

Assuming that the number of preformed deuterons φ has a rather small value and $Z' \approx A'/2$ one can obtain, approximately

$$F_d \cong \frac{2\varphi\sigma_{xd}}{\sigma_{xp} + \sigma_{xn}}. \tag{13}$$

For the evaluation of the cross-section ratio in Eq. (13) the cross-section of the free elastic nucleon-deuteron scattering was taken from ENDF/B-VI at the energy up to 150 MeV and evaluated above 150 MeV using the data from EXFOR. The free nucleon-nucleon interaction cross-sections were obtained from Ref. [24]. The σ_{xd}, σ_{xp} and σ_{xn} cross-sections were calculated taking into account the limitation superimposed by the Pauli principle on the number of intranuclear interactions. It was assumed, that the angular distribution of interacting particles is approximately isotropic in the center-of-mass system. The Fermi energy for deuterons was taken equal to $2E_F$.

Fig. 2 shows the ratio of the cross-sections $\sigma_{xd}/(\sigma_\omega\pi + \sigma_{\omega\xi})$ at the different kinetic energy of the incident nucleon calculated for the nuclear potential well with the Fermi energy equal to 32 MeV. The ratio for the free nucleon-deuteron and free nucleon-nucleon scattering cross-sections is also shown.

The obtained value of $\sigma_{xd}/(\sigma_{xp} + \sigma_{xn})$ for the nuclear potential well (Fig. 2) was approximated as follows

$$\frac{\sigma_{xd}}{\sigma_{xp} + \sigma_{xn}} = 0.512\exp(-9.81\cdot 10^{-3}E_p), \tag{14}$$

where E_p is the kinetic energy of projectile outside of the nucleus in MeV units.

Eq. (10–11) and (13–14) were used in the present work for the calculation of the knock-out component of deuteron precompound spectra.

Fig. 1 shows the calculated contribution of the deuteron knock-out in the deuteron emission spectrum for ^{54}Fe and ^{197}Au irradiated with 61.5 MeV protons. Parameters used for the calculation are discussed in Sect. 2.5.

2.3 Multiple pre-equilibrium emission

The multiple particle emission gives a noticeable contribution in precompound emission spectra of composite particles forming in nuclear reactions induced by nucleons with energies above 50 MeV [21, 22].

The multiple pre-equilibrium effect is taken into account for the deuteron emission as described below. The pick-up and coalescence contributions for the spectrum of deuterons escaping after the pre-equilibrium emission of nucleons are calculated by the following expression

$$\frac{d\sigma_2^{F-U,C}}{d\varepsilon_d} = \pi\lambda^2\sum_{l=0}^{\infty}(21+1)\mathrm{T}_1\sum_{x=\pi,\nu}^{2}\int_{E_x^{\min}}^{E_x^{\max}}$$

$$\times\sum_{n=n_0}{}_nX_x\frac{\omega(p-1,h,E-Q_x-\varepsilon_x)}{\omega(p,h,E)}$$

$$\times\frac{\lambda_x^e(\varepsilon_x)}{\lambda_x^e(\varepsilon_x)+\lambda_x^+(\varepsilon_x)}gD(n)$$

$$\times\sum_{n'=p+h-1}\sum_{k+m=2}F_{k,m}(\varepsilon_d+Q_d{}')$$

$$\times\frac{\omega(p'-k,h',E-Q_x-\varepsilon_x-Q_d'-\varepsilon_d)}{\omega(p',h',E-Q_x-\varepsilon_x)}$$

$$\times\frac{\lambda_d^e(\varepsilon_d)}{\lambda_d^e(\varepsilon_d)+\lambda_d^+(\varepsilon_d)}g_dD_2(n')d\varepsilon_x \tag{15}$$

where λ is the reduced de Broglie wavelength of the incident particle; T_1 is the transmission coefficient for 1$^{\text{th}}$ partial wave; ${}_nX_x$ is the number of nucleons of *x*-type in the n-exciton state; *"x"* refers to proton and neutron emitted; Q_x is the separation energy for nucleon in the composite nucleus; ε_x is the channel energy for x-particle; Q_d' is the separation energy for deuteron in the nucleus formed after the emission of nucleon of *x*-type; $E_x^{\min}$ and $E_x^{\max}$ define the energy range, where the emission of the *x*-particle occurs; D_2 is the depletion factor concerning the escape of particles from n'-exciton state.

The analogous formula is written for the deuteron knock-out following the fast nucleon emission. The successive emission of three and more pre-equilibrium particles is not considered here.

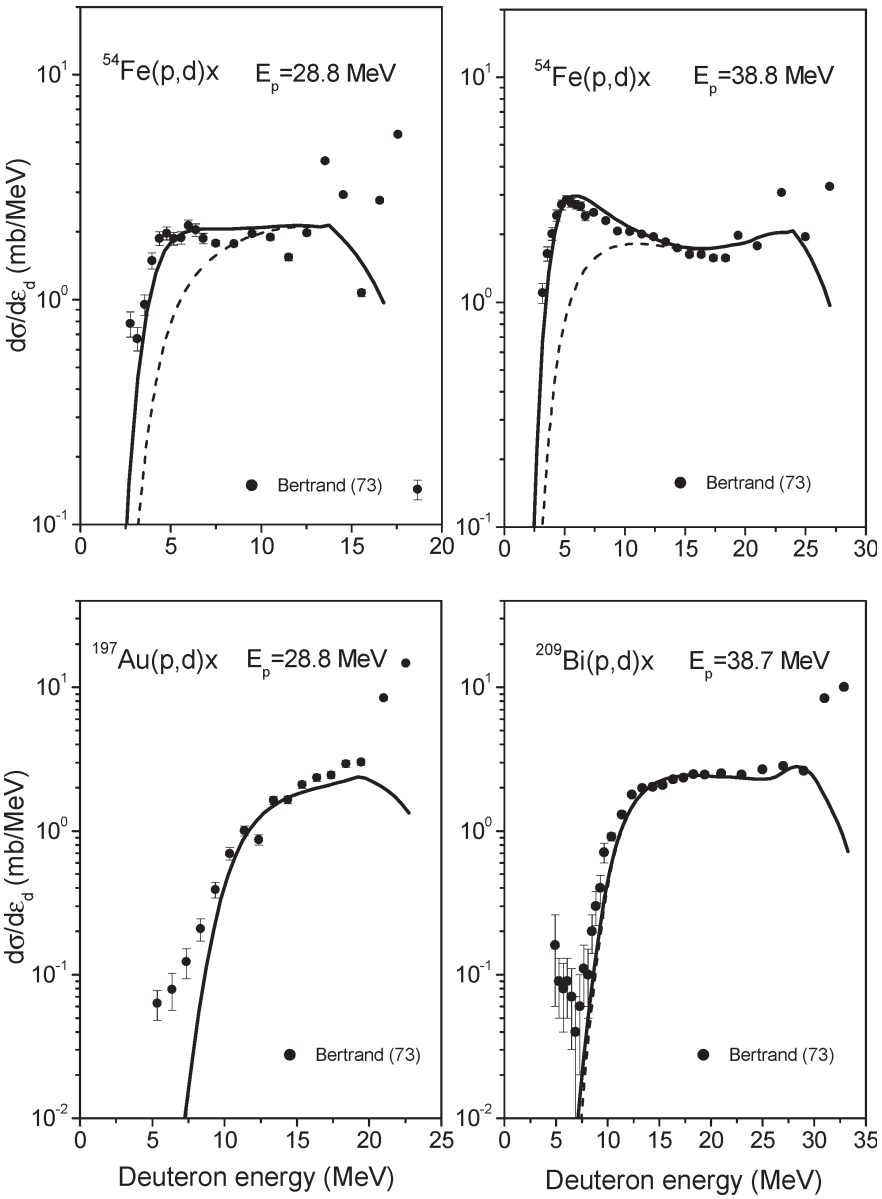

Fig. 10. Calculated total deuteron emission spectrum (solid line) and nonequilibrium deuteron emission spectrum (dashed line) for $p + {}^{54}Fe$, $p + {}^{197}Au$ and $p + {}^{209}Bi$ reactions induced by protons with the energy from 28.8 to 38.8 MeV. Experimental data are taken from Ref. [12]

Fig. 3 shows the contribution of the multiple pre-equilibrium emission in calculated energy distribution of deuterons emitted.

2.4 Direct pick-up process

The process corresponds to the pick-up of nucleon without formation of the (2p, 1h) exciton configuration. The final state is (0p, 1h). The rigorous description of this process can be done only outside the pre-equilibrium theory. However, the mathematical expressions obtained formally with the help of the precompound exciton model [1, 5] are used for the phenomenological and qualitative description of the direct nucleon pick-up.

According to Ref. [1] the direct component of the deuteron spectrum is

$$\frac{d\sigma^D}{d\varepsilon_d} = \sigma_{non}\frac{\omega^*(U)}{\omega(1p,0h,E)}\frac{\lambda_d^e(\varepsilon_d)}{\lambda_d^e(\varepsilon_d)+\lambda_d^+(\varepsilon_d)}g_d, \tag{16}$$

where the final level density $\omega^*(U)$ is approximated in Ref. [1] by $\omega(0p,1h,U)\cdot\gamma/g_d$ with the γ value equal to $2\cdot10^{-3}$ MeV^{-1} for all nuclei and excitation energies.

The formal consideration of the finite depth of the nuclear potential well shows that Eq. (16) can contribute only in the most high energy part of the deuteron emission spectrum, as it has been mentioned above. In this case the calculated part of the spectrum is a rectangular step with the width equal to E_F. To improve the agreement of calculations and the measured deuteron spectra it is useful to write the direct component of the spectrum in the following form

$$\frac{d\sigma^D}{d\varepsilon_d} = \sigma_{non}\,\alpha_1\exp\left(-\frac{(E-\alpha_2E_F)^2}{2(\alpha_3E_F)^2}\right)\frac{\lambda_d^e(\varepsilon_d)}{\lambda_d^e(\varepsilon_d)+\lambda_d^+(\varepsilon_d)}g_d, \tag{17}$$

where α_1, α_2 and α_3 are parameters, E_F is the effective value of the Fermi energy.

The values of $\alpha_{\rm i}$ can be obtained from the analysis of experimental deuteron spectra (Sect. 2.5). The global parameterization of $\alpha_{\rm i}$ parameters is hardly possible.

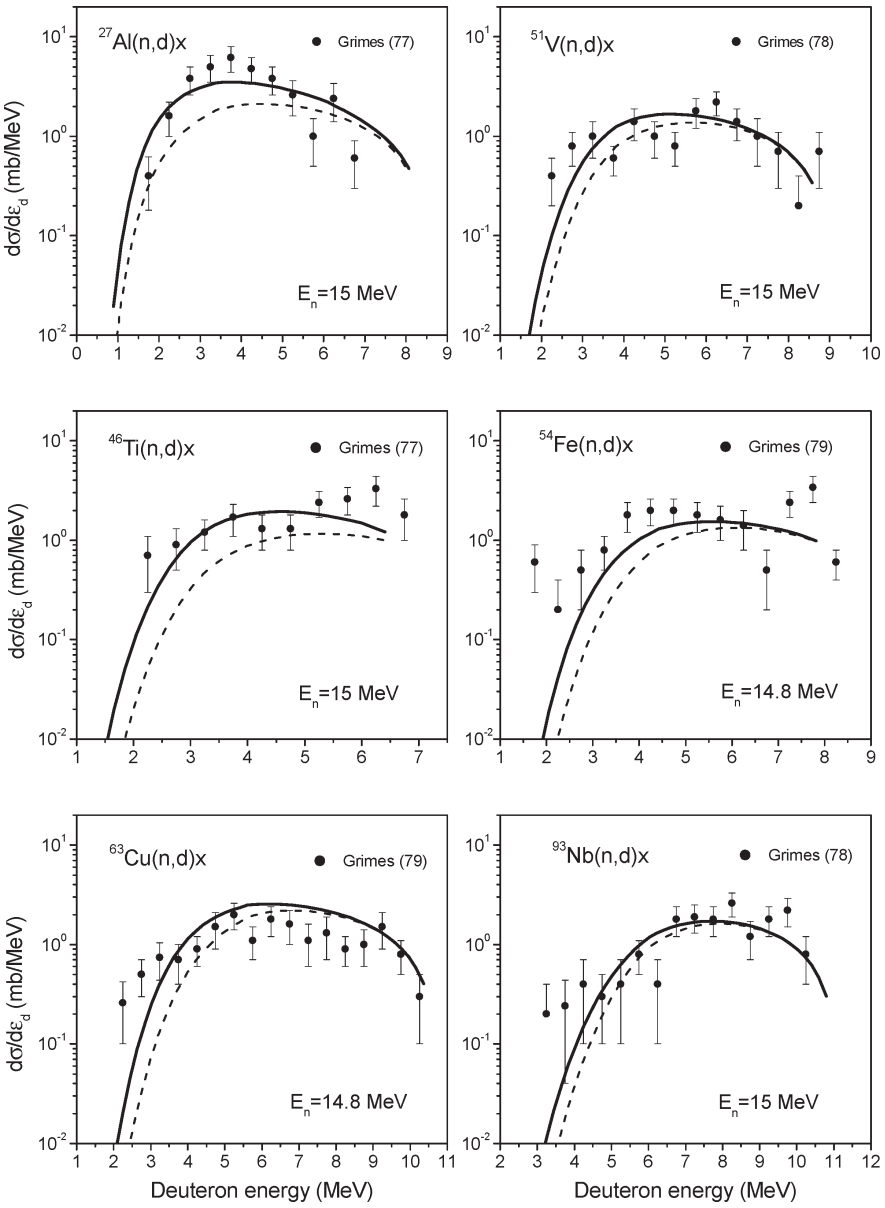

Fig. 11. Calculated total deuteron emission spectrum (solid line) and nonequilibrium deuteron emission spectrum (dashed line) for a number of neutron induced reactions at the incident neutron energy 14.8 and 15 MeV Experimental data are taken from Refs. [28–30]

Fig. 1 shows the $d\sigma^D/d\varepsilon_d$ component of the calculated deuteron spectrum for ^{54}Fe(p,d)x and ^{197}Au(p,d)x reactions induced by 61.5 MeV protons.

2.5 Parameters of the model

Model parameters were obtained from the comparison of calculations with the experimental data [12, 13, 16, 25–30]. The deuteron spectra were calculated using Eq. (1)–(11), (13)–(15), (17).

The change in values of different parameters results to the different energetic dependence of calculated deuteron spectrum. In most cases such change cannot be represented by simple redefinition of other model parameters.

The global normalization of the sum for the $F_{1,1}$ pick-up and the $F_{2,0}$ coalescence components adopted in Ref. [1] was kept unchanged

$$\sum_{k+m=2} F_{k,m} = 0.3 \qquad (18)$$

The single particle state density for deuteron g_d was taken equal to $g/2$.

The φ parameter of the knock-out model obtained from the comparison of the experimental data and calculations for different nuclei is equal to 0.18 ± 0.03.

The effective value of the Fermi energy E_F was found equal to 5 MeV. This rather small value reflects the influence of surface nuclear effects on the deuteron emission. The similar reduction of the effective Fermi energy was obtained from the analysis of nucleon pre-equilibrium spectra in Refs. [18, 19]. Fig. 4 shows the influence of the effective E_F value on the calculated deuteron energy distribution.

The imaginary part of the optical potential W_d^{opt} was parameterized as follows $W_d^{opt} = W_0$ at $\varepsilon_d < \varepsilon_1$ and $W_d^{opt} = W_0 \cdot \exp(\beta \cdot (\varepsilon_d - \varepsilon_1))$ at $\varepsilon_d \geq \varepsilon_1$; $W_0 = \gamma_1 \cdot (E_1 - E_p) + W_1$ at $E_p \leq E_1$, $W_0 = \gamma_2 \cdot (E_p - E_1) + W_1$ at $E_p > E_1$ and $W_0 = \gamma \cdot (E_2 - E_1) + W_1$ at $E_p > E_2$, where $\varepsilon_1 = 20$ MeV, $\beta = -0.1027 \cdot \exp(-11.45 \cdot (A - 2Z)/A)$, $E_1 = 62$ MeV, $E_2 = 90$ MeV, $\gamma_1 = -1.37 \cdot 10^{-3}$A $- 0.213, \gamma 2 = -0.45$, $W1 = 32$ MeV. This rather complex energy and A- dependence of W_d^{opt} results from the fitting of calculations to experimental deuteron spectra.

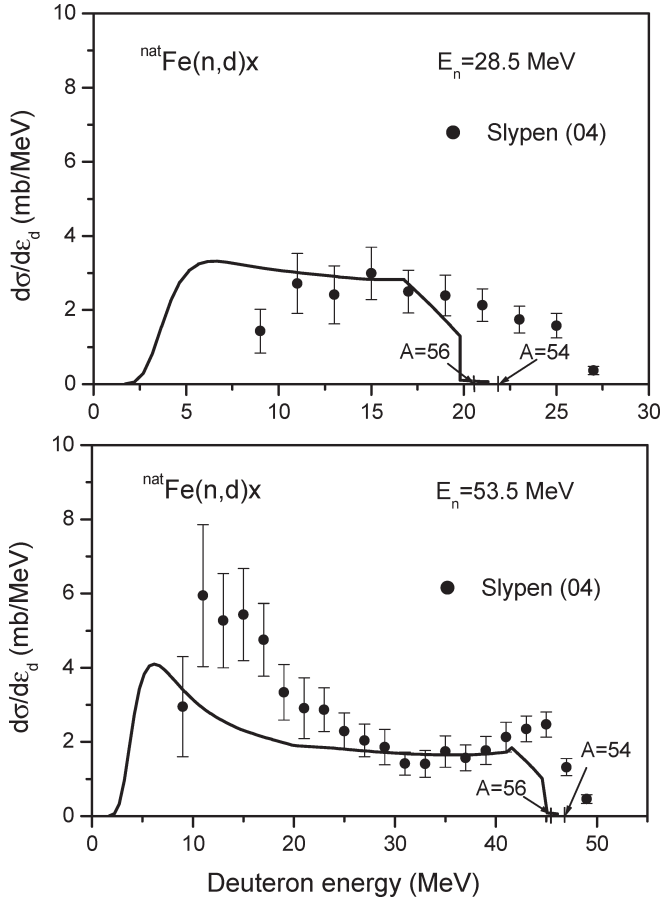

Fig. 12. Calculated deuteron emission spectra for Fe(n,d)x reaction induced by 28.5 and 53.5 MeV neutrons (solid line). The maximal energy of deuterons for ^{54}Fe(n,d) and ^{56}Fe(n,d) reactions is shown by touches on the x-axis. Experimental data are taken from Ref. [9, 41]

Partly, it accumulates an uncertainty of different measurements and reflects general approximate character of the model discussed.

The parameters of Eq. (17) have been obtained from the analysis of the experimental data. For the most nuclei the value of α_1 is equal to $1.5 \cdot 10^{-3}$. The α_2 parameter value is equal to 0.77 ± 0.54 and α_3 is equal to 0.52 ± 0.18. It is supposed that E_F is equal to 5 MeV in Eq. (17).

The inverse reaction cross-sections have been calculated as described in Refs. [31, 32]. The optical potential of Koning and Delaroche [33] has been used for the calculation of the cross-section of nonelastic interactions, σ_{non} for primary neutrons and protons.

The numerical calculations were performed with the help of the modified version of the ALICE/ASH code [34, 35].

The model parameters used for the computation of nucleon precompound spectra make an influence on the calculated energy distribution of deuterons. The nucleon spectra were calculated using the geometry dependent hybrid model [4]. The results of calculations were compared with the experimental data [12, 13, 16, 27, 28, 36, 37] for several nuclei from ^{27}Al to ^{209}Bi. The comparison shows that in most cases the measured nucleon spectra are described by model calculations with the multiplication factor for the free nucleon path in the nucleus [4, 31, 34, 35] equal to one. For the incident nucleon energy above 90 MeV the factor of two has been adopted.

3 Comparison of calculations with experimental data

The calculation of deuteron energy distributions has been carried out using Eq. (1)–(11), (13)–(15), (17) with the help of the ALICE/ASH code.

Figs. 5–7 shows the deuteron emission spectra calculated for nuclei from ^{12}C to ^{209}Bi irradiated with 61.5–62.9 MeV protons. The deuteron energy distributions calculated for reactions induced by 90 MeV protons and 96 MeV neutrons are shown in Figs. 8–9. The experimental data presented in Figs. 5–8 are taken from Refs. [12, 13, 16, 27]. There is an agreement between calculated and measured spectra.

Examples of deuteron emission spectra calculated for nuclear reactions induced by nucleons of lower energies are shown in Figs. 10–11. The reasonable agreement is observed for calculations and experimental data [12, 28–30].

Recently a large number of measurements [37–41] has been made for charge particle emission spectra in neutron induced reactions. A special comment is required concerning deuteron distributions obtained in Refs. [37–41]. The comparison of model calculations with the experimental data shows a large discrepancy at the high energy tail of measured deuteron spectra [9]. Partly experimental points are in kinematically forbidden energy region. The authors [9] mentioned that it results from the measurement technique concerning i) the energy resolution of the incident neutron spectrum, ii) the flat neutron energy distribution at lower incident neutron energy used in measurements.

The comparison of present calculations with the experimental data [9, 41] also shows a noticeable difference. It is more obvious at lower projectile energy, where the experimental points are above the kinematic limit of the reaction. Fig. 12 shows the calculated deuteron spectrum for n+^{nat}Fe reaction at the projectile energy 28.5 and 53.5 MeV. The small step in the high energy part of calculated spectra is due to the ^{54}Fe(n,d) reaction contribution. The isotope ^{54}Fe has the highest value of the (n,d) reaction energy ($Q_{n,d} = -6.63$ MeV) comparing with other stable iron isotopes ($Q_{n,d}$: ^{56}Fe: -7.96, ^{57}Fe: -8.335, ^{58}Fe: -9.73 MeV). The maximal energy of deuterons corresponding to ^{54}Fe(n,d) and ^{56}Fe(n,d) reactions are shown by touches on the energy axis (Fig. 12). Fig. 12 shows that the measured deuteron spectra are partly above the kinematic limit of the (n,d) reaction. At the lower incident neutron energy (28.5 MeV) the discrepancy between the calculated high energy part of the spectrum and the measured data is more evident. The lacks of measurements mentioned above make a rather questionable to test theoretical models of deuteron emission using the data discussed at least at lower incident neutron energies.

4 Conclusion

A phenomenological model is proposed for the non-equilibrium deuteron emission in nuclear reactions induced by nucleons of intermediate energies. The model combines the model of the nucleon pick-up, the coalescence and the deuteron knock-out.

The model of Sato, Iwamoto, Harada [2, 3] is used to describe the nucleon pick-up and the nucleon coalescence from exciton states starting from the (2p, 1h) configuration. The probability of the nucleon interaction with "preformed" deuterons in the knock-out model is calculated taking into account the Pauli principle. The contribution of the direct pick-

up is described phenomenologically. The multiple pre-equilibrium emission of deuterons (the precompound deuteron escape after the fast nucleon emission) is considered. The emission and absorption rates of excited particles are calculated by the hybrid model [4]. The exciton level density is calculated taking into account the finite depth of the nuclear potential depth.

The calculated deuteron energy distributions are in reasonable agreement with measured data.

(Received on 8 August 2005)

References

1 *Konobeyev, A. Yu.; Korovin, Yu. A.:* Calculation of deuteron spectra for nucleon induced reactions on the basis of the hybrid exciton model taking into account direct processes. Kerntechnik 61 (1996) 45

2 *Iwamoto, A.; Harada, K.:* Mechanism of cluster emission in nucleon-induced preequilibrium reactions. Phys. Rev. C 26 (1982) 1821

3 *Sato, K.; Iwamoto, A.; Harada, K.:* Pre-equilibrium emission of light composite particles in the framework of the exciton model. Phys. Rev. C 28 (1983) 1527

4 *Blann, M.; Vonach, H. K.:* Global test of modified precompound decay models. Phys. Rev. C 28 (1983) 1475

5 *Kalbach, C.:* The Griffin model, complex particles and direct nuclear reactions. Z. Phys. A283 (1977) 401

6 *Korovin, Yu. A.; Konobeyev, A. Y.; Pereslavtsev, P. E.; Stankovsky, A. Y.; Broeders, C.; Broeders, I.; Fischer, U.; von Möllendorff, U.; Wilson, P.; Woll, D.:* Evaluation and test of nuclear data for investigation of neutron transport, radiation damage and processes of activation and transmutation in materials irradiated by intermediate and high energy particles. Proc. Int. Conf. Nuclear Data for Science and Technology, Trieste, Italy, May 1997, p. 851; Progress in Nuclear Energy 40 (2002) 673

7 *Chadwick, M. B.; Young, P. G.; Chiba, S.; Frankle, S. C.; Hale, G. M.; Hughes, H. G.; Koning, A. J.; Little, R. C. ; MacFarlane, R. E.; Prael, R. E.; Waters L. S.:* Cross-section evaluations to 150 MeV for accelerator-driven systems and implementation in MCNPX. Nucl. Sci. Eng. 131 (1999) 293

8 *Kalbach Walker, C.:* PRECO-2000: Exciton Model Preequilibrium Code with Direct Reactions, Triangle Universities Nuclear Laboratory, Duke University, Durham, March 2001; http://www.nndc.bnl.gov/nndcscr/model-codes/preco-2000/index.html

9 *Slypen, I.; Nica, N.; Koning, A.; Raeymackers, E.; Benck, S.; Meulders, J. P.; Corcalciuc, V.:* Light charged particle emission induced by fast neutrons with energies between 25 and 65 MeV on iron. J. Phys. G: Nucl. Part. Phys. 30 (2004) 45

10 *Raeymackers, E.; Benck, S.; Nica, N.; Slypen, I.; Meulders, J. P.; Corcalciuc, V.; Koning, A.:* Light charged particle emission in fast neutron (25–65 MeV) induced reactions on ^{209}Bi. Nucl. Phys. A726 (2003) 210

11 *Raeymackers, E.; Benck, S.; Slypen, I.; Meulders, J. P.; Nica, N.; Corcalciuc, V.; Koning, A.:* Light charged particle production in the interaction of fast neutrons (25–65 MeV) with uranium nuclei. Phys. Rev. C68 (2003) 024604

12 *Bertrand, F. E.; Peelle, R. W.:* Complete hydrogen and helium particle spectra from 30- to 60-MeV proton bombardment of nuclei with A = 12 to 209 and comparison with the intranuclear cascade model. Phys. Rev. C 8 (1973) 1045

13 *Wu, J. R.; Chang, C. C.; Holmgren, H. D.:* Charged-particle spectra: 90 MeV protons on ^{27}Al, ^{58}Ni, ^{90}Zr, and ^{209}Bi. Phys. Rev. C 19 (1979) 698

14 *Sultana, S. A.; Syafarudin ■; Aramaki, F.; Maki, D.; Wakabayashi, G.; Uozumi, Y.; Ikeda, N.; Matoba, M.; Watanabe, Y.; Sen Gupta, H. M.:* Analysis of continuum spectra of (n,d) reactions with direct reaction model. Proc. of the 2003 Symposium on Nuclear Data, JAERI, Tokai, Japan, November 27–28, 2003; http://wwwndc.tokai.jaeri.go.jp/nds/proceedings/2003/ contents.html

15 *Ribanský, I.; Obložinský, P.:* Emission of complex particles in the exciton model, Phys. Lett. 45B (1973) 318

16 *Blideanu, V.; Lecolley, F. R.; Lecolley, J. F.; Lefort, T.; Marie, N.; Ataç, A.; Ban, G.; Bergenwall, B.; Blomgren, J.; Dangtip, S.; Elmgren, K.; Eudes, Ph.; Foucher, Y.; Guertin, A.; Haddad, F.; Hildebrand, A.; Johansson, C.; Jonsson, O.; Kerveno, M.; Kirchner, T.; Klug, J.; Le Brun, Ch.; Lebrun, C.; Louvel, M. ; Nadel-Turonski, P.; Nilsson, L.; Olsson, N.; Pomp, S.; Prokofiev, A. V.; Renberg, P.-U.;. Rivière, P.-U.; Slypen, I.; Stuttgé, L.; Tippawan, U.; Österlund, M.:* Nucleon-induced reactions at intermediate energies: New data at 96 MeV and theoretical status. Phys. Rev. C 70 (2004) 014607

17 *Běták, E.; Dobeš, J.:* The finite depth of the nuclear potential well in the exciton model of preequilibrium decay. Z. Phys. A 279 (1976) 319

18 *Kalbach, C.*: Surface and collective effects in preequilibrium reactions. Phys. Rev. C 62 (2000) 044608; Phys. Rev. C 64 (2001) 039901(E)

19 *Kalbach, C.*: Surface effects in preequilibrium reactions of incident neutrons. Phys. Rev. C 69 (2004) 014605

20 *Dimitrova, S. S.; Krumova, G. Z.; Hodgson, P. E.; Avrigeanu, V.; Antonov, A. N.:* (n,d)-reactions on medium mass nuclei. J. Phys. G: Nucl. Part. Phys. 23 (1997) 961

21 *Konobeyev, A. Yu.; Lunev, V. P.; Shubin, Yu. N.:* Pre-equilibrium emission of clusters. Acta Physica Slovaca 45 (1995) 705

22 *Broeders, C. H. M.; Konobeyev, A. Yu.:* Evaluation of ^{4}He production cross-section for tantalum, tungsten and gold irradiated with neutrons and protons at the energies up to 1 GeV. To be published in Nucl. Instr. Meth. B (2005)

23 *Obložinský, P; Ribanský, I.:* Emission rate of preformed α particles in preequilibrium decay. Phys. Lett. 74B (1978) 6

24 *Chen, K.; Fraenkel, Z.; Friedlander, G.; Grover, J. R.; Miller, J. M.; Shimamoto, Y.:* VEGAS: A Monte Carlo simulation of intranuclear cascades. Phys. Rev. 166 (1968) 949

25 *Bateman, F. B.; Haight, R. C.; Chadwick, M. B.; Sterbenz, S. M.; Grimes, S. M.; Vonach, H.:* Light charged-particle production from neutron bombardment of silicon up to 60 MeV: Role of level densities and isospin. Phys. Rev. C 60 (1999) 064609

26 *Duisebayev, A.; Ismailov, K. M.; Boztosun, I.:* Inclusive spectra of (p,xp) and (p,xd) reactions on ^{90,92}Zr and ^{92}Mo nuclei at $E_p = 30.3$ MeV. Phys. Rev. C 67 (2003) 044608

27 *Guertin, A.; Marie, N.; Auduc, S.; Blideanu, V.; Delbar, Th.; Eudes, P.; Foucher, Y.; Haddaa, F.; Kirchner, T.; Koning, A. J.; Lebrun, Ch.; Lebrun, C.; Lecolley, F. R.; Lecolley, J. F.; Ledoux, X.; Lefebvres, F.; Louvel, M.; Ninane, A.; Patin, Y.; Pras, Ph.; Riviere, G.; Varignon, C.:* Neutron and light charged particle productions in proton induced reactions on Pb-208 at 62.9-MeV. EXFOR O1146015

28 *Grimes, S. M.; Haight, R. C.; Anderson, J. D.:* Measurement of sub-Coulomb-barrier charged particles emitted from A1 and Ti bombarded by 15-MeV neutrons. Nucl. Sci. Eng. 62 (1977) 187

29 *Grimes, S. M.; Haight, R. C.; Anderson, J. D.:* Charged-particle-producing reactions of 15-MeV neutrons on ^{51}V and ^{93}Nb. Phys. Rev. C 17 (1978) 508

30 *Grimes, S. M.; Haight, R. C.; Alvar, K. R.; Barschall, H. H.; Borchers, R. R.:* Charged-particle emission in reactions of 15-MeV neutrons with isotopes of chromium, iron, nickel, and copper. Phys. Rev. C 19 (1979) 2127

31 *Blann, M.:* ALICE-91: Statistical model code system with fission competition. RSIC CODE PACKAGE PSR-146

32 *Shubin, Yu. N.; Lunev, V. P.; Konobeyev, A. Yu.; Dityuk, A. I.:* Cross-section library MENDL-2 to study activation and transmutation of materials irradiated by nucleons of intermediate energies. INDC(CCP)-385, International Atomic Energy Agency Report, Iss. 1995

33 *Koning, A. J.; Delaroche, J. P.:* Local and global nucleon optical models from 1 keV to 200 MeV. Nucl. Phys. A713 (2003) 231; data are taken from http://ndswebserver.iaea.org/RIPL-2/

34 *Konobeyev, A. Yu.; Korovin, Yu. A.; Pereslavtsev, P. E.:* Code ALICE/ASH for calculation of excitation functions, energy and angular distributions of emitted particles in nuclear reactions. Obninsk Institute of Nuclear Power Engineering, Iss. 1997

35 *Dityuk, A. I.; Konobeyev, A. Yu.; Lunev, V. P.; Shubin, Yu. N.:* New advanced version of computer code ALICE-IPPE. INDC(CCP)-410, International Atomic Energy Agency Report, Iss. 1998

36 *Kalend, A. M.; Anderson, B. D.; Baldwin, A. R.; Madey, A. R.; Watson, J. W.; Chang, C. C.; Holmgren, H. D.; Koontz, R. W.; Wu, J. R.: Machner, H.:* Energy and angular distributions of neutrons from 90 MeV proton and 140 MeV alpha-particle bombardment of nuclei. Phys. Rev. C 28 (1983) 105

37 *Slypen, I.; Benck, S.; Meulders, J. P.; Corcalciuc, V.:* Experimental cross sections for light charged particle production induced by neutrons with energies between 25 and 75 MeV incident on carbon. Atomic Data and Nuclear Data Tables 76 (2000) 26

38 *Benck, S.; Slypen, I.; Meulders, J. P.; Corcalciuc, V.:* Experimental cross sections for light-charged particle production induced by neutrons with energies between 25 and 65 MeV incident on oxygen. Atomic Data and Nuclear Data Tables 72 (1999) 1

39 *Benck, S.; Slypen, I.; Meulders, J. P.; Corcalciuc, V.:* Experimental cross sections for light-charged particle production induced by

neutrons with energies between 25 and 65 MeV incident on aluminum. Atomic Data and Nuclear Data Tables 78 (2001) 161

40 *Benck, S.; Slypen, I.; Meulders, J.-P.; Corcalciuc, V.:* Secondary Light Charged Particle Emission from the Interaction of 25- to 65-MeV Neutrons on Silicon. Nucl. Sci. Eng. 141 (2002) 55

41 *Raeymackers, E.; Slypen, I.; Benck, S.; Meulders, J. P., Nica, N.; Corcalciuc, V.:* Experimental cross-sections for light charged particle emission induced by neutrons with energies between 25 and 65 MeV incident on ^{nat}Fe, ^{59}Co, ^{209}Bi, and ^{nat}U. Atomic Data and Nuclear Data Tables 87 (2004) 231

The authors of this contribution

C. H. M. Broeders and *A. Yu. Konobeyev*[*], Institut für Reaktorsicherheit, Forschungszentrum Karlsruhe GmbH, 76021, Karlsruhe, Germany.

[*]Corresponding author: E-mail: konobeev@irs.fzk.de